

FRESNEL ZONES IN GRIN MEDIA

José Manuel Rivas-Moscoso, Carlos Gómez-Reino, and María Victoria Pérez

Laboratorio de Óptica, Departamento de Física Aplicada, Facultade de Física
and Escola de Óptica e Optometría, Universidade de Santiago de Compostela
Campus Sur, E15782 Santiago de Compostela, Spain

Phone/Fax: (+34) 981521984 E-mail: moskeh@usc.es / facgrc@usc.es

ABSTRACT

The free propagation of a wavefront in an inhomogeneous medium with parabolic refractive index profile and the division of the wavefront into Fresnel zones are studied. We determine the radius and the area of each zone as well as the zone contribution to the total wave at an observation point inside the medium. We find the condition that the optical path must fulfill from each zone to the aforementioned point so that the disturbance due to successive zones will be in phase opposition. Once this condition is settled the concept of zone plate in gradient-index (GRIN) media can be introduced.

Keywords: Gradient-index, light propagation

1. INTRODUCTION

Fresnel zones resulting from the division of a wavefront that propagates in a homogeneous medium are well known in optics and have received widespread attention. Fundamental properties and many practical applications have been considered [1]. The purpose of this work is to generalize the zone division of a wavefront for inhomogeneous media [2]. The study will be restricted to the propagation of light in a GRIN medium and to the evaluation of the contribution of the successive zones to the total disturbance at a point.

2. FREE PROPAGATION OF A WAVEFRONT IN AN INHOMOGENEOUS MEDIUM

Let us consider a tapered GRIN medium characterized by a transverse parabolic refractive index modulated by an axial index and whose refractive index profile is given by

$$n^2(x, z) = n_0^2 [1 - g^2(z) \cdot r^2]; \quad r^2 = x^2 + y^2, \quad (1)$$

where n_0 is the index at the z optical axis and $g(z)$ is the taper function that describes the evolution of the transverse parabolic index distribution along the z axis.

A point source situated at the input of the medium emits light that propagates a distance z , producing a disturbance at a point (r_0, z) which can be expressed as

$$\psi(r_0; z) = \frac{kn_0}{2\pi i H_1(z)} \exp(ikn_0 z) \exp\left\{i \frac{kn_0}{2H_1(z)} [r_0^2 \dot{H}_1(z)]\right\}, \quad (2)$$

where $H_1(z)$ and $\dot{H}_1(z)$ are the position and the slope of the axial ray [3], the dot indicating differentiation with respect to z . From this equation the curvature radius can be defined as $R(z) = H_1(z)/[n_0 \dot{H}_1(z)]$.

The complex amplitude distribution at a point (r, z') —see Fig.1— can be calculated from the wavefront in Eq. (2) by solving the diffraction integral [3]

$$\psi(r; z') = \int_{\Sigma} K(r, r_0; z') \psi(r_0; z) d\Sigma, \quad (3)$$

where $K(r, r_0; z')$ is the expression of the propagator in cylindrical coordinates

$$K(r, r_0; z') = \frac{-ikn_0}{2\pi H_1(z')} \exp[ikn_0(z' - z)] \exp\left\{\frac{ikn_0}{2H_1(z')} [\dot{H}_1(z')r^2 + H_2(z')r_0^2 - 2rr_0 \cos(\varphi - \theta)]\right\}, \quad (4)$$

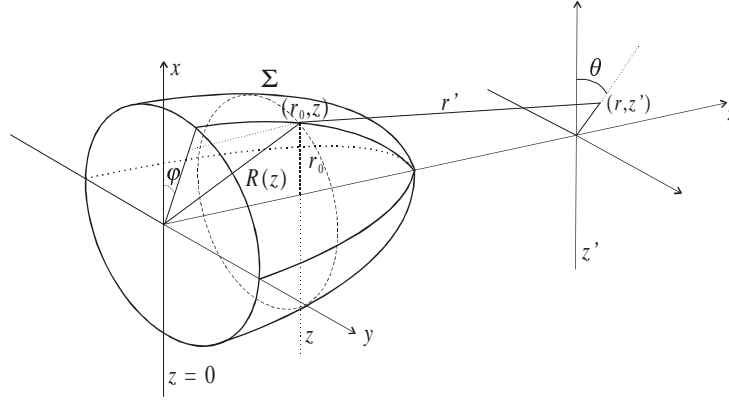


Figure 1. Geometry for the propagation and division of a wavefront in a GRIN medium.

$d\Sigma$ is the surface element and $H_1(z')$, $H_2(z')$, $\dot{H}_1(z')$ and $\dot{H}_2(z')$ are, respectively, the position and the slope of the axial and field ray at z' after propagating from z .

Substitution of Eqs. (2) and (4) into Eq. (3) provides

$$\begin{aligned} \psi(r; z') = & - \int_{\Sigma} \frac{k^2 n_0^2}{4\pi^2 H_1(z) H_1(z')} \exp(ikn_0 z') \exp\left\{i \frac{kn_0}{2H_1(z')} \dot{H}_1(z') r^2\right\} \exp\left\{i \frac{kn_0}{2H_1(z)} \dot{H}_1(z) r_0^2\right\} \\ & \times \exp\left\{i \frac{kn_0}{2H_1(z')} H_2(z') r_0^2\right\} \exp\left\{-i \frac{kn_0}{H_1(z')} r r_0 \cos(\varphi - \theta)\right\} d\Sigma. \end{aligned} \quad (5)$$

In order to divide the wavefront into zones, we consider a circular aperture with radius h and assume slow variations of z within the zone determined by this aperture. Furthermore, we restrict the study to wavefronts sufficiently far from the planes where $H_1(z) = 0$ (image planes) –which allows us to develop the surface element in power series— and to observation points on the optical axis. With these conditions in mind, Eq. (5) becomes

$$\psi(z') = \int_0^h \zeta(z, z') \exp\left\{i \frac{B(z, z')}{2} r_0^2\right\} \left[1 + \frac{1}{2} \frac{\dot{H}_1^2(z)}{H_1^2(z)} r_0^2\right] r_0 dr_0, \quad (6)$$

whose solution is

$$\psi(z') = \frac{\zeta(z, z')}{iB(z, z')} \left\{ \left[\exp\left(i \frac{B(z, z')}{2} h^2\right) - 1 \right] + \frac{\dot{H}_1^2(z)}{2H_1^2(z)} \left[h^2 \exp\left(i \frac{B(z, z')}{2} h^2\right) - \frac{2}{iB} \left[\exp\left(i \frac{B(z, z')}{2} h^2\right) - 1 \right] \right] \right\} \quad (7)$$

and where we have defined

$$\zeta(z, z') = - \frac{k^2 n_0^2}{2\pi H_1(z') H_1(z)} \exp\{ikn_0 z'\} \exp\left\{i \frac{kn_0}{2H_1(z')} \dot{H}_1(z') r^2\right\}, \text{ and } B(z, z') = kn_0 \left(\frac{\dot{H}_1(z)}{H_1(z)} + \frac{H_2(z')}{H_1(z')} \right). \quad (8)$$

For a better understanding of the end-result we will analyze the following two cases: $\dot{H}_1(z)$ equal to zero and $\dot{H}_1(z)$ small in comparison to $H_1(z)$, which will be discussed below.

2.1. Wavefront at Fourier Transform Planes

At the Fourier transform planes ($\dot{H}_1(z) = 0$) the wavefront curvature becomes zero and, consequently, no variations of z within a zone are present. This fact allows the second addend to be deleted in Eq. (7), being the field and the irradiance given, respectively, by

$$\psi_{TF}(z') = \frac{\zeta(z, z')}{iB(z, z')} \left\{ \exp\left[i \frac{B(z, z')}{2} h^2\right] - 1 \right\}; \quad I_{TF}(z') = \frac{k^2 n_0^2}{\pi^2 H_1^2(z) H_2^2(z')} \sin^2 \left[\frac{B(z, z')}{4} h^2 \right], \quad (9)$$

and we can find the values of h for which maxima and minima of irradiance are reached at a point z' as well as the distances r_j from z' to the upper part of the zones defined by those values of h . These distances r_j are

$$r_j = (z' - z) + \frac{j\lambda H_1(z')}{2n_0 H_2(z')(z' - z)}, \quad (10)$$

where j is an integer which assumes an even value for minima and an odd value for maxima.

Nonetheless, the presence of the inhomogeneous medium induces a shift of the maxima, resulting in the principal maximum always being located at planes verifying $H_1(z') = 0$ (imaging planes) and the secondary maxima slightly shifting from the resulting positions of Eq. (10). The minima do not show any displacement at all.

2.2. Wavefront off Fourier Transform Planes

When the wavefront is moved off the Fourier transform planes, with the restriction $\dot{H}_1(z) \ll H_1(z)$, the term in Eq. (7) that goes with B^2 is very small and can be disregarded, being the irradiance at a point z'

$$I(z') = \frac{k^2 n_0^2}{\pi^2 [\dot{H}_1(z)H_1(z') + H_2(z')H_1(z)]^2} \sin^2 \left[\frac{B(z, z')}{4} h^2 \right] \left\{ 1 + \frac{h^2 \dot{H}_1^2(z)}{2H_1^2(z)} \right\}. \quad (11)$$

In this case, the distances r_j become

$$r_j = (z' - z) + \frac{j\lambda H_1(z')R(z)}{2(z' - z)[n_0 H_2(z')R(z) + H_1(z')]}, \quad (12)$$

where, again, the maxima are shifted, but now the principal maximum is not exactly at the imaging planes. In Fig.2 we represent the displacement of the principal maximum from the imaging planes against the displacement of the wavefront from the Fourier transform planes. We observe a change in the position of the principal maximum which is dependent on the particular conditions of the problem. As the wavefront shifts from the Fourier transform planes, the principal maximum moves away from the imaging planes and subsequently approaches them again. The maximum shift from the imaging planes is, however, achieved for the same wavefront location in all cases, which leads us to conclude that the maximum shift is only a function of the medium characteristics.

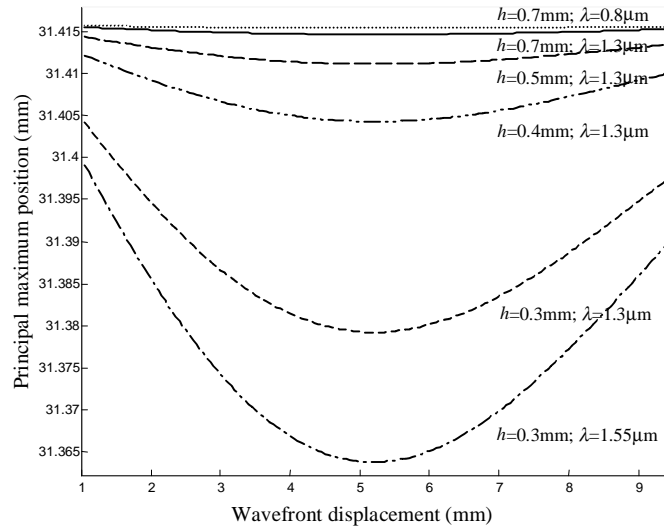


Figure 2. Displacement of the principal maximum from the imaging planes as a function of the displacement of the wavefront from the Fourier transform planes. For our calculations the first imaging plane is at $z' = 10\pi$ mm.

3. ZONE RADII AND AREAS

Using Eqs. (10) and (12) and with a simple geometric calculation, we can determine the radii of every zone into which the wavefront has been divided for wavefronts at Fourier planes and off them. The expressions for the two cases are, respectively

$$h_j^2 = \frac{j\lambda H_1(z')}{n_0 H_2(z')} ; \quad h_j^2 = \frac{j\lambda H_1(z') H_1(z)}{n_0 [H_2(z') H_1(z) + H_1(z') \dot{H}_1(z)]} . \quad (13)$$

In the same way, integrating the surface element $d\Sigma$ within the limits of each zone, we can determine the zone areas, which are given by

$$\Sigma_j = \frac{\pi\lambda H_1(z')}{n_0 H_2(z')} ; \quad \Sigma_j = \frac{\pi\lambda H_1(z') H_1(z)}{n_0 [H_2(z') H_1(z) + H_1(z') \dot{H}_1(z)]} . \quad (14)$$

These expressions duplicate the classic results for homogeneous media [4] by making $H_1(z') \rightarrow z' - z$ and $H_2(z') \rightarrow 1$.

4. ZONE CONTRIBUTION TO THE TOTAL DISTURBANCE

Equation (6) allowed us to determine the total disturbance at a point z' due to a circular aperture of radius h . To find the contribution of a single zone, we only have to change the integration limits. Hence, for wavefronts at Fourier transform planes and off them, the contribution of the j th zone to the field at z' is given, respectively, by

$$\psi_j(z') = (-1)^{j-1} \frac{2i\zeta(z, z')}{B(z, z')} ; \quad \psi_j(z') = (-1)^{j-1} \frac{2i\zeta(z, z')}{B(z, z')} \left[1 - \frac{\dot{H}_1^2(z)}{2B(z, z') H_1^2(z)} (\pi - j2\pi - 2i) \right] . \quad (15)$$

We note that the contributions of the successive zones are alternately positive and negative. The total effect at z' is obtained by summing all these contributions. If j is odd a minimum is obtained at z' and if j is even the irradiance will give a maximum. For wavefronts at Fourier transform planes all the zones contribute in the same way, whereas the contributions are slightly different for wavefronts shifted from that plane.

CONCLUSIONS

We have divided a wavefront into periodic zones by calculating the difference in optical path between successive zones. We have determined the radii and the areas of those zones, obtaining that they coincide for each zone when the wavefront is situated at a Fourier transform plane. Once this done, we have obtained the disturbance produced by these zones separately at a point on the optical axis, noticing that their contributions are alternately positive and negative. The fact that successive zones provoke contributions to the total disturbance which tend to cancel each other out implies that we would observe a huge increase in the irradiance at a point if we eliminate all the even or odd zones. This suggests and justifies the construction of zone plates in GRIN media, which will be the next step in our study.

ACKNOWLEDGMENTS

This work has been supported by the Xunta de Galicia, Spain, under contract PGIDT99PXI22201B.

REFERENCES

- [1] J. Ojeda-Castañeda, and C. Gómez-Reino, eds., *Selected Papers on Zone Plates*, SPIE Mileston Series, MS 128, 1996.
- [2] Yu. A. Kravtsov, and Yu. I. Orlov, *Geometrical Optics of Inhomogeneous Media*, Springer-Verlag, Berlin, 1990.
- [3] J. M. Rivas-Moscoso, C. Gómez-Reino, C. Bao, and M. V. Pérez, "Tapered gradient-index media and zone plates," *J. Mod. Optics* **47**, pp. 1549-1567, 2000.
- [4] M. Born, and E. Wolf, *Principles of Optics*, University Press, Cambridge, 1997.